LA-UR-17-20814
Approved for public release; distribution is unlimited.

Title: (U) An Analytic Examination of Piezoelectric Ejecta Mass Measurements

Author(s): Tregillis, Ian Lee

Intended for: Proceedings of the 2016 Nuclear Explosives Code Design Conference (NECDC), held Oct. 17-21, 2016 at Lawrence Livermore National Laboratory in Livermore, CA, USA.

Issued: 2017-02-02

(U) An Analytic Examination of Piezoelectric Ejecta Mass Measurements

I. L. Tregillis[1]

[1]iant@lanl.gov
Los Alamos National Laboratory, Los Alamos, New Mexico

Abstract

Ongoing efforts to validate a Richtmyer-Meshkov instability (RMI) based ejecta source model [1, 2, 3] in LANL ASC codes use ejecta areal masses derived from piezoelectric sensor data [4, 5, 6]. However, the standard technique for inferring masses from sensor voltages implicitly assumes instantaneous ejecta creation [7], which is not a feature of the RMI source model. To investigate the impact of this discrepancy, we define separate "areal mass functions" (AMFs) at the source and sensor in terms of typically unknown distribution functions for the ejecta particles, and derive an analytic relationship between them. Then, for the case of single-shock ejection into vacuum, we use the AMFs to compare the analytic (or "true") accumulated mass at the sensor with the value that would be inferred from piezoelectric voltage measurements. We confirm the inferred mass is correct when creation is instantaneous, and furthermore prove that when creation is not instantaneous, the inferred values will always overestimate the true mass. Finally, we derive an upper bound for the error imposed on a perfect system by the assumption of instantaneous ejecta creation. When applied to shots in the published literature, this bound is frequently less than several percent. Errors exceeding 15% may require velocities or timescales at odds with experimental observations.

1 Introduction

We consider the problem of measuring the areal mass of an ejecta cloud through the use of a piezoelectric sensor, specifically in the situation where ejecta production is the result of a single shock, and where all transport between the source and sensor occurs in vacuum. This analysis does not apply to double-shock experiments, nor to cases where the ejecta are transported through a gaseous medium. The present treatment assumes negligible deceleration of the free surface during an extended ejecta creation interval, although the situation may differ in the case of an unsupported shock.

We begin in Section 2 by defining the problem geometry and establishing several fundamental relationships. Then we derive the fundamental equation governing coordinate transformations

between the source (i.e., free-surface) and sensor (i.e., laboratory) rest frames. This enables us to derive expressions for both the analytic ("true") and measured ("inferred") accumulated ejecta mass at the sensor, for any given analytic function describing the time- and velocity-dependent areal mass at the source. In Section 3, we use these results to derive a general expression for the error, χ. This leads to a simple upper bound on the error percentage imposed (on a perfect system) by the assumption of instantaneous ejecta creation. This bound arises strictly from kinematic considerations; it does not rely upon assumptions about the velocity or size distributions of the ejecta particles.

Finally, in Section 4, we apply this general result to eight shots from the published literature.

2 Definitions and derivations

We begin by introducing all definitions, conventions, and derivations used throughout this analysis.

2.1 Kinematics

All definitions are derived from the problem geometry depicted in Fig. 1.

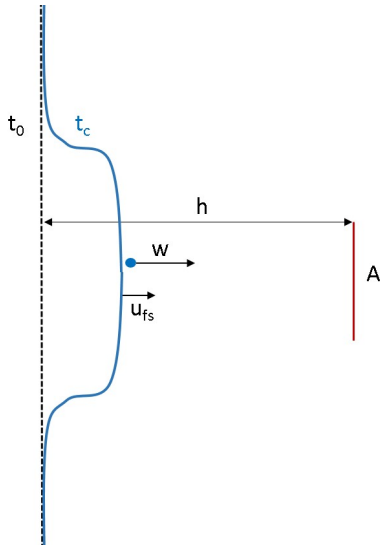

Figure 1: Cartoon depiction of the problem geometry. The dashed line (black) represents the initial (unperturbed) free surface at the shock breakout time, t_0. The solid line (blue) represents the free surface at the creation time (t_c) for a given particle of interest, which is born with velocity w *relative to the free surface*. The free surface is assumed to undergo instantaneous acceleration to constant velocity u_{fs} at the instant of shock breakout. The known initial distance from the unperturbed free surface to the piezoelectric sensor (with collecting area A) is h. (All calculations in this treatment assume a uniformly accelerated free surface.)

Let us define the shock breakout time (t_0), the time of ejecta particle creation (t_c), and the time of particle arrival at the sensor (t). Our convention is that velocities measured relative to the free surface are denoted w, and that velocities measured relative to the motionless sensor (i.e., in the lab frame) are denoted u. The free surface velocity in the lab frame is u_{fs} (assumed constant in this treatment). A particle with velocity w relative to the free surface has velocity $u = w + u_{fs}$ relative to the sensor. We define all times and velocities to be positive, and only consider times prior to the arrival of the free surface at the sensor.

For a particle created (i.e., ejected from the free surface) at time t_c with relative velocity w, the arrival time at the sensor, t, will be given by

$$t\left(w, t_c\right) = t_c + \frac{h - u_{fs}\left(t_c - t_0\right)}{w + u_{fs}} = \frac{wt_c + \left(h + u_{fs}t_0\right)}{w + u_{fs}}. \tag{1}$$

This is simply the creation time plus the transit time from the free surface location at time t_c to the static pin location; $u_{fs}(t_c - t_0)$ is the distance traveled by the free surface between the shock breakout and particle creation times. (Notice that when $t_c = t_0$ (i.e., when the ejecta particle is created at the instant of shock breakout) the arrival time is the creation time plus the time of flight; when $t_c = t_0 = 0$, the arrival time is simply the time of flight.) From this we can obtain the creation time, t_c, required for a particle with relative velocity w to arrive at the sensor at time t:

$$t_c\left(w, t\right) = \frac{\left(w + u_{fs}\right)t - \left(h + u_{fs}t_0\right)}{w}. \tag{2}$$

Both $t\left(w, t_c\right)$ and $t_c\left(w, t\right)$ can be converted to functions of lab-frame velocity, u, via the substitution $w = u - u_{fs}$. The lab-frame velocity required such that a particle created at time t_c arrives at the sensor at a specified time t is straightforward:

$$u\left(t_c, t\right) = \frac{h - u_{fs}\left(t_c - t_0\right)}{t - t_c} \tag{3}$$

from which we obtain the associated relative velocity:

$$w\left(t_c, t\right) \equiv u\left(t_c, t\right) - u_{fs} = \frac{h - u_{fs}\left(t_c - t_0\right)}{t - t_c} - u_{fs} = \frac{h - u_{fs}\left(t - t_0\right)}{t - t_c}. \tag{4}$$

Note that Eqns. 1 and 2 imply that for a *fixed* velocity, w,

$$\frac{dt}{dt_c} = \left(\frac{w}{w + u_{fs}}\right) = \left(\frac{u - u_{fs}}{u}\right) \tag{5}$$

$$\frac{dt_c}{dt} = \left(\frac{w + u_{fs}}{w}\right) = \left(\frac{u}{u - u_{fs}}\right). \tag{6}$$

Consider particles of a fixed relative velocity w, emitted continuously during a creation interval Δt_c. Their arrival interval at the sensor, Δt, will be shorter than Δt_c because the free surface approaches the sensor during the emission interval, meaning particles emitted later in the interval travel a shorter distance at the same velocity than particles emitter earlier in the interval. Thus $\Delta t_c > \Delta t$ for a fixed velocity.

2.2 Distribution functions and areal mass functions

Microphysics at the free surface determines, either explicitly or implicitly, a distribution function for the ejecta particles. In particular, we define

$$f_c\left(m, w, t_c\right) \mathrm{d}m \, \mathrm{d}w \, \mathrm{d}t_c \tag{7}$$

to be the number of ejecta particles created during the time interval $[t_c, t_c + \mathrm{d}t_c]$ with mass in the range $[m, m + \mathrm{d}m]$ and relative velocity in the range $[w, w + \mathrm{d}w]$. Then it follows

$$\iiint f_c\left(m, w, t_c\right) \mathrm{d}m \, \mathrm{d}w \, \mathrm{d}t_c = N_t \tag{8}$$

where N_t is the total number of ejecta particles created at the free surface, and thus

$$f_c = \frac{\mathrm{d}N\left(m, w, t_c\right)}{\mathrm{d}m \, \mathrm{d}w \, \mathrm{d}t_c} \tag{9}$$

where $N\left(m, w, t_c\right)$ is the number of ejecta particles created at time t_c with mass m and relative velocity w. The units of f_c must be $\left[\mathrm{mass}^{-1} \cdot \mathrm{velocity}^{-1} \cdot \mathrm{time}^{-1}\right]$ or $\left[\mathrm{mass}^{-1} \cdot \mathrm{length}^{-1}\right]$.

The total ejecta mass is given by

$$\iiint m f_c\left(m, w, t_c\right) \mathrm{d}m \, \mathrm{d}w \, \mathrm{d}t_c = M_t \tag{10}$$

so

$$\int m f_c\left(m, w, t_c\right) \mathrm{d}m = \frac{\mathrm{d}M}{\mathrm{d}w \, \mathrm{d}t_c} \tag{11}$$

where $M\left(w, t_c\right)$ is the ejecta mass created at time t_c with relative velocity w.

We can now define the *areal mass function* for particles of relative velocity w created at the time t_c:

$$m_c\left(w, t_c\right) \equiv \frac{1}{A} \int m f_c\left(m, w, t_c\right) \mathrm{d}m. \tag{12}$$

The units of m_c are $\left[\mathrm{mass} \cdot \mathrm{area}^{-1} \cdot \mathrm{velocity}^{-1} \cdot \mathrm{time}^{-1}\right]$ or $\left[\mathrm{mass} \cdot \mathrm{volume}^{-1}\right]$.

Similar reasoning may be applied to the distribution function, f_a, of particles arriving at the piezoelectric sensor in the lab frame. In that fashion we obtain the areal mass function for particles of lab-frame velocity u arriving (collected) at time t:

$$m_a\left(u, t\right) \equiv \frac{1}{A} \int m f_a\left(m, u, t\right) \mathrm{d}m. \tag{13}$$

The lab-frame areal mass function m_a has the same units as m_c.

Because m_c is determined by microphysics of ejecta production at the free surface, it is defined in the rest frame of the free surface. Alternatively, because m_a is determined by the distribution of ejecta particles arriving at the sensor, it is most sensible to define that function in the lab frame.

Note furthermore that specific knowledge of the distribution functions f_c and f_a is unnecessary for our purposes. It is sufficient to know the areal mass functions can be related to the microphysics of ejecta production via the (possibly unknown) distribution functions.

2.3 Relationship between $\mathrm{m_a}$ and $\mathrm{m_c}$

Our goal is to investigate how reliably quantities inferred from sensor measurements reflect the true (analytic) situation. To do that, we must first derive a relationship between m_a and m_c.

We assume all ejecta particles created at the free surface eventually arrive at the sensor, and that the motion is collinear so that the relevant area does not change. (See [7] for a full description of the assumptions underlying the piezoelectric sensor analysis.) Thus a particle arriving at the detector at time t with lab-frame velocity u must have been created at the free surface with relative velocity $w = u - u_{fs}$ at time $t_c\left(u - u_{fs}, t\right)$. We therefore expect

$$m_a\left(u,t\right) \propto m_c\big[u - u_{fs}, t_c\left(u - u_{fs}, t\right)\big].$$

Mass conservation implies

$$m_a\left(u,t\right)\mathrm{d}u\,\mathrm{d}t = m_c\left(w,t_c\right)\mathrm{d}w\,\mathrm{d}t_c$$

or

$$m_a\left(u,t\right) = \frac{\mathrm{d}w}{\mathrm{d}u}\frac{\mathrm{d}t_c}{\mathrm{d}t}m_c\left(w,t_c\right) = \left(\frac{w+u_{fs}}{w}\right)m_c\left(w,t_c\right),$$

from which we obtain the fundamental equation relating the source (m_c) and sensor (m_a) areal mass functions:

$$m_a\left(u,t\right) = \left(\frac{u}{u-u_{fs}}\right)m_c\left[u-u_{fs}, \frac{ut-(h+u_{fs}t_0)}{u-u_{fs}}\right]. \tag{14}$$

Eqn. 14 can be confirmed by computing the total ejecta mass created at the free surface and collected at the sensor. Conservation of mass requires

$$A\int_0^\infty\int_0^\infty m_c\left(w,t_c\right)\mathrm{d}w\,\mathrm{d}t_c = A\int_0^\infty\int_0^\infty m_a\left(u,t\right)\mathrm{d}u\,\mathrm{d}t.$$

Applying Eqn. 14 and the substitutions

$$x = u - u_{fs} \qquad y = \frac{ut-(h+u_{fs}t_0)}{u-u_{fs}}$$

to the right-hand expression (the total mass collected at the sensor) yields

$$\begin{aligned} &A\int_0^\infty\int_0^\infty \left(\frac{u}{u-u_{fs}}\right)m_c\left[u-u_{fs}, \frac{ut-(h+u_{fs}t_0)}{u-u_{fs}}\right]\mathrm{d}u\,\mathrm{d}t \\ &= A\int_{-u_{fs}}^\infty\int_{-\frac{h+u_{fs}t_0}{u-u_{fs}}}^\infty \left(\frac{x+u_{fs}}{x}\right)m_c\left(x,y\right)\left(\frac{x}{x+u_{fs}}\right)\mathrm{d}x\,\mathrm{d}y. \end{aligned}$$

Because the problem is defined such that all velocities and times are positive, $m_c\left(x,y\right) = 0$ for both $x < 0$ and $y < 0$. Thus the right-hand expression becomes

$$A\int_0^\infty\int_0^\infty m_c\left(x,y\right)\mathrm{d}x\,\mathrm{d}y$$

which is exactly equivalent to the left-hand expression (the total mass ejected by the free surface). This demonstates that mass is conserved.

Thus, Eqn. 14 is the correct relationship between the areal mass functions at the source and sensor.

2.4 Pressure and accumulated areal mass

We can now write expressions for the time-dependent pressures on the free surface and the sensor, and for the time-dependent accumulated areal mass at the sensor, given an areal mass function at the source.

The pressure on the free surface is equivalent to the recoil momentum flux. This is simply

$$P_c\left(t_c\right) = \int_0^\infty m_c\left(w, t_c\right) w \, \mathrm{d}w. \tag{15}$$

Similarly, the pressure on the sensor is given by

$$P\left(t\right) = \int_0^\infty m_a\left(u, t\right) u \, \mathrm{d}u = \int_0^\infty \left(\frac{u^2}{u - u_{fs}}\right) m_c\left[u - u_{fs}, \frac{ut - \left(h + u_{fs}t_0\right)}{u - u_{fs}}\right] \mathrm{d}u. \tag{16}$$

The *analytic* ("true") mass per unit area accumulated at the sensor is clearly

$$m_t(t) = \int_0^t \mathrm{d}t' \int_0^\infty m_a\left(u, t'\right) \mathrm{d}u \tag{17}$$

(note this becomes the total accumulated mass as $t \to \infty$). We choose this form for simplicity, although clearly $m_t(t) = 0$ for $0 < t < t_0^a$ where t_0^a is the earliest particle arrival time at the sensor; likewise, of course, $m_a(u, t) = 0$ for $u \leq u_{fs}$.

Meanwhile, and as derived in [7] by assuming all ejecta particles are created at the instant of shock breakout, the accumulated ejecta mass per unit area *inferred* from the piezoelectric sensor measurement is

$$m_i(t) = \int_0^t \left(\frac{t' - t_0}{h}\right) P\left(t'\right) \, \mathrm{d}t' = \frac{1}{h} \int_0^t \mathrm{d}t' \int_0^\infty m_a(u, t') \, u \left(t' - t_0\right) \mathrm{d}u \tag{18}$$

where $P(t)$ is the pressure measured by the sensor, i.e., Eqn. 16. The preceding observation regarding the integration limits applies here, as well: we choose this form for simplicity, although both lower limits of integration could be increased to positive values without changing the evaluation.

Eqns. 15 - 18 embody everything we need to examine the piezoelectric mass measurement procedure analytically for any test problem defined by a known source areal mass function $m_c(w, t_c)$. It is worth noting, however, that this treatment also enables us to compute an analytic expression for the time-dependent voltage at the pin. As explained in [7], the pin voltage is given by

$$V(t) = A \, R \, S \, \frac{\mathrm{d}P}{\mathrm{d}t} \tag{19}$$

where $P(t)$ is again given by Eqn. 16, R is the terminating resistance of the circuit, and S is the piezoelectric sensitivity.

2.5 Time-dependent u_{fs}

Throughout, this treatment assumes the free-surface velocity to be constant. Here we comment briefly on the situation $u'_{fs}(t_c) \neq 0$.

In this case, the distance traveled by the free surface between times t_0 and t_c is

$$\Delta h = \int_{t_0}^{t_c} u_{fs}(t'_c)\,\mathrm{d}t'_c,$$

and thus

$$t\,(w, t_c) = t_c + \frac{h - \displaystyle\int_{t_0}^{t_c} u_{fs}(t'_c)\,\mathrm{d}t'_c}{w + u_{fs}(t_c)}. \tag{20}$$

This leads to

$$\begin{aligned}\frac{\mathrm{d}t}{\mathrm{d}t_c} &= 1 - \frac{u_{fs}(t_c)}{w + u_{fs}(t_c)} - u'_{fs}(t_c) \cdot \frac{h - \displaystyle\int_{t_0}^{t_c} u_{fs}(t'_c)\,\mathrm{d}t'_c}{\left[w + u_{fs}(t_c)\right]^2} \\ &= \frac{w}{w + u_{fs}(t_c)} - u'_{fs}(t_c) \cdot \frac{h - \displaystyle\int_{t_0}^{t_c} u_{fs}(t'_c)\,\mathrm{d}t'_c}{\left[w + u_{fs}(t_c)\right]^2}. \end{aligned} \tag{21}$$

When u_{fs} is constant, this reduces to Eqn. 1. When u_{fs} is decreasing, Δt increases relative to Δt_c, which matches our expectations: it is the motion of the free surface which leads to the compressed interval at the sensor relative to the source, so if the free surface becomes motionless, the source and sensor intervals will become equivalent. Conversely, if u_{fs} is increasing, then the arrival interval relative to the creation interval will become even shorter than that obtained for the case of a constant u_{fs}.

Given a known $u_{fs}(t_c)$, Eqn. 20 cannot be solved algebraically for t_c. The entire treatment for this scenario becomes nonalgebraic.

In situations where the free surface is driven by an unsupported shock (e.g., a Taylor wave), u_{fs} may indeed decrease during the ejecta creation period. However, the present formulation can still be used to estimate the errors in the piezoelectric mass measurement (see Section 3) by computing $\chi(t)$ (see Eqn. 22) for both $u_{fs} = u_{fs}(t_0)$ and $u_{fs} = \min(u_{fs})$.

3 General expression for the error in the inferred areal mass, χ

It is straightforward to derive an expression for $\chi(t)$, the ratio of the inferred accumulated areal mass to the true accumulated areal mass, for *any* areal mass function $m_c(w, t_c)$.

Recall, from Eqn. 17, that the true accumulated areal mass at the sensor is

$$m_t(t) = \int_0^t \mathrm{d}t' \int_0^\infty m_a(u, t')\,\mathrm{d}u$$

while from Eqn. 18 the inferred accumulated areal mass at the sensor is

$$\begin{aligned} m_i(t) = \int_0^t \left(\frac{t' - t_0}{h}\right) P(t')\,\mathrm{d}t' &= \int_0^t \mathrm{d}t' \left(\frac{t' - t_0}{h}\right) \int_0^\infty m_a(u, t') u\,\mathrm{d}u \\ &= \frac{1}{h} \int_0^t \mathrm{d}t' \int_0^\infty m_a(u, t')\,u\,t'\,\mathrm{d}u, \end{aligned}$$

where for simplicity, and with no loss of generality, we have set $t_0 = 0$. We now apply Eqn. 14 to write these areal masses as functions of m_c rather than m_a. When $t_0 = 0$, the true accumulated areal mass becomes

$$m_t(t) = \int_0^t \mathrm{d}t' \int_0^\infty \left(\frac{u}{u - u_{fs}}\right) m_c\left(u - u_{fs}, \frac{ut' - h}{u - u_{fs}}\right) \mathrm{d}u.$$

Let $x \equiv u - u_{fs}$ (which is clearly w, but to avoid confusion we simply define x as a variable with units of velocity). Then

$$m_t(t) = \int_0^t \mathrm{d}t' \int_{-u_{fs}}^\infty \left(\frac{x + u_{fs}}{x}\right) m_c\left[x, \frac{(x + u_{fs})t' - h}{x}\right] \mathrm{d}x.$$

Now let $y \equiv \frac{(x+u_{fs})t'-h}{x}$. (Clearly, $y = t_c(w, t')$. But as with x, we treat y merely as a convenient substitution variable.) Note there is no problem with y diverging at $x = 0$: ejecta particles can only arrive at the sensor when $u > u_{fs} \implies x > 0$ (see Section 2.4 regarding the limits of integration). Then

$$\begin{aligned} m_t(t) &= \int_{-u_{fs}}^\infty \mathrm{d}x \int_{-\frac{h}{x}}^{\frac{(x+u_{fs})t-h}{x}} \left(\frac{x + u_{fs}}{x}\right) m_c(x, y) \left(\frac{x}{x + u_{fs}}\right) \mathrm{d}y \\ &= \int_0^\infty \mathrm{d}x \int_0^{t_c(x,t)} m_c(x, y)\, \mathrm{d}y \end{aligned}$$

This expression makes sense. It's the integral of the areal mass function at the source over the *creation* interval that corresponds to the *arrival* interval ending at time t.

The inferred areal mass at the sensor is

$$m_i(t) = \frac{1}{h} \int_0^t \mathrm{d}t' \int_0^\infty \left(\frac{u}{u - u_{fs}}\right) m_c\left(u - u_{fs}, \frac{ut' - h}{u - u_{fs}}\right) u\, t'\, \mathrm{d}u.$$

Let us apply the same substitution variables, x and y, from above. Now

$$ut' = (x + u_{fs}) \cdot \left(\frac{xy + h}{x + u_{fs}}\right) = xy + h,$$

and thus

$$\begin{aligned} m_i(t) &= \frac{1}{h} \int_{-u_{fs}}^\infty \mathrm{d}x \int_{-\frac{h}{x}}^{\frac{(x+u_{fs}t)-h}{x}} \left(\frac{x + u_{fs}}{x}\right) m_c(x, y)\, (xy + h) \left(\frac{x}{x + u_{fs}}\right) \mathrm{d}y \\ &= \frac{1}{h} \int_0^\infty \mathrm{d}x \int_0^{t_c(x,t)} m_c(x, y)(xy + h)\, \mathrm{d}y \\ &= \int_0^\infty \mathrm{d}x \int_0^{t_c(x,t)} m_c(x, y)\, \mathrm{d}y + \frac{1}{h} \int_0^\infty \mathrm{d}x \int_0^{t_c(x,t)} m_c(x, y)\, x\, y\, \mathrm{d}y \\ &= m_t(t) + \frac{1}{h} \int_0^\infty \mathrm{d}x \int_0^{t_c(x,t)} m_c(x, y)\, x\, y\, \mathrm{d}y. \end{aligned}$$

We therefore find that for *any* given areal mass function at the source, $m_c(w, t_c)$, the ratio of inferred to true accumulated areal mass at the sensor is

$$\frac{m_i(t)}{m_t(t)} \equiv \chi(t) = 1 + \frac{1}{h} \cdot \frac{\displaystyle\int_0^\infty \mathrm{d}x \int_0^{t_c(x,t)} m_c(x, y)\, x\, y\, \mathrm{d}y}{\displaystyle\int_0^\infty \mathrm{d}x \int_0^{t_c(x,t)} m_c(x, y)\, \mathrm{d}y}$$

or

$$\chi(t) = 1 + \frac{1}{h} \cdot \frac{\int_{w_0}^{w_1} \int_0^{t_c(w,t)} w\, t_c\, m_c(w, t_c)\, \mathrm{d}t_c\, \mathrm{d}w}{\int_{w_0}^{w_1} \int_0^{t_c(w,t)} m_c(w, t_c)\, \mathrm{d}t_c\, \mathrm{d}w}$$

where $t_0 = 0$ for simplicity, $t_c(w,t) = \frac{(w+u_{fs})t-h}{w}$, and we have denoted the minimum and maximum relative velocities by w_0 and w_1, respectively. Note $t_c(w, t_c) \geq 0 \implies w \geq \frac{h}{t} - u_{fs}$. Finally, then, we have

$$\boxed{\chi(t) = 1 + \frac{1}{h} \cdot \frac{\int_{\frac{h}{t}-u_{fs}}^{w_1} \int_0^{t_c(w,t)} w\, t_c\, m_c(w, t_c)\, \mathrm{d}t_c\, \mathrm{d}w}{\int_{\frac{h}{t}-u_{fs}}^{w_1} \int_0^{t_c(w,t)} m_c(w, t_c)\, \mathrm{d}t_c\, \mathrm{d}w}}. \tag{22}$$

For sufficiently large arrival times, t, (such as when evaluating the $\chi(t)$ at the end of the arrival period) the lower bound on the velocity integral will fall below w_0, at which point it can be replaced with w_0.

Note that Eqn. 22 is the error imposed *on a perfect system* by the assumption of instantaneous ejecta creation. The overall error in the inferred mass will be higher in a real measurement, owing to noise and other effects.

We have defined the problem such that $m_c \geq 0$, $w \geq 0$, and $t_c \geq 0$. This means $\chi(t) \geq 1$ for all arrival times t, which in turn means that for a perfect system *the piezoelectric sensor analysis can never underestimate the ejecta mass*. By assuming all particles are launched instantaneously, the piezo analysis implicitly interprets later-arriving particles as being slower but heavier to achieve the same impulse. So the analysis skews toward larger ejecta masses later in the arrival period.

The error percentage, P, is

$$\frac{100}{h} \cdot \frac{\int_{\frac{h}{t}-u_{fs}}^{w_1} \int_0^{t_c(w,t)} w\, t_c\, m_c(w, t_c)\, \mathrm{d}t_c\, \mathrm{d}w}{\int_{\frac{h}{t}-u_{fs}}^{w_1} \int_0^{t_c(w,t)} m_c(w, t_c)\, \mathrm{d}t_c\, \mathrm{d}w},$$

so for the error level to exceed $P\%$ requires

$$\frac{100}{hP} \cdot \int_{\frac{h}{t}-u_{fs}}^{w_1} \int_0^{t_c(w,t)} w\, t_c\, m_c(w, t_c)\, \mathrm{d}t_c\, \mathrm{d}w > \int_{\frac{h}{t}-u_{fs}}^{w_1} \int_0^{t_c(w,t)} m_c(w, t_c)\, \mathrm{d}t_c\, \mathrm{d}w. \tag{23}$$

Consider the quantity $\frac{100}{hP} w t_c$. If this were exactly unity over the entire integration domain, then the left and right sides of Eqn. 23 would be identically equal. If this quantity were less than unity over the entire integration domain, then the integrand of the left side would be less than the integrand of the right side at every point in the domain. Because all quantities are nonnegative for this problem, that would guarantee the quantity on the left is less than the quantity on the right. Therefore, the inequality in Eqn 23 can only be satisfied if

$$\frac{100}{hP} w t_c > 1 \qquad \text{or} \qquad w t_c > \frac{hP}{100}$$

over at least some portion of the integration domain (which is a function of t).

Each P value therefore defines a curve in the (w, t_c) plane; this curve must intersect the integration domain in order for the error percentage to exceed $P\%$. (Intersection is a necessary but not sufficient condition.) Clearly then, there is a maximum error percentage, P_{max}, such that the curves for $P > P_{max}$ never intersect the integration domain. A simple estimate for P_{max} is

$$P_{max} = \max\ 100 \cdot \frac{w}{h} \cdot t_c$$

where the maximum is computed over the domain of integration. A straightforward value for this bound uses the maximum ejecta relative velocity, w_1, and the final creation time, t_{cf} (or the duration of the creation interval, $t_{cf} - t_0$, if $t_0 \neq 0$). (This is an estimate because particles of velocity w_1 might not be emitted at time t_{cf}, if the velocity distribution defined by $m_c(w, t_c)$ is nonstationary.) Finally, then, the weakest upper bound on the error percentage is

$$P_{max} = 100\frac{w_1 t_{cf}}{h}. \tag{24}$$

(Interestingly, this is the simplest first-order quantity that one might construct from dimensional analysis and a consideration of how the error might be expected to scale with the pin distance and creation time.) For experiments where h is known from the configuration and u_{fs} and $u_{ej} \equiv u_1 = w_1 + u_{fs}$ are measured, this sets an upper bound on the error as a function of the creation interval.

For a given arrival time, t, the integration domain is the region of the (w, t_c) plane bounded by the inequalities

$$\frac{h}{t} - u_{fs} \leq w \leq w_1 \qquad 0 \leq t_c \leq \frac{(w + u_{fs})t - h}{w}.$$

The portion of this domain where $wt_c > \frac{hP}{100}$ is that part of the domain above the line $t_c = \frac{hP}{100w}$. This is represented schematically in Fig. 2, as is the contour for $P = P_{max}$. In order for the integration domain to contain points with $wt_c > \frac{hP}{100}$, the creation interval must extend to times

$$t_c > \frac{hP}{100w_1}.$$

As an example, the parameter values explored in Shot 6 of [4] yield $\frac{h}{w_1} \approx 32.4$ μs, meaning the upper bound on the error will be approximately 3% unless the creation interval exceeds 1 microsecond (see Section 4).

3.1 Instantaneous creation

If all ejecta are created instantaneously at the moment of shock breakout, the areal mass function at the source will have the form

$$m_c(w, t_c) = g(w)\delta(t_c - t_0) = g(w)\delta(t_c)$$

when $t_0 = 0$. Because $m_c = 0$ for $t_c < 0$, the lower limit of integration over t_c in Eqn. 22 may be extended to any negative value, thereby forcing the numerator to zero and yielding $\chi(t) = 1$. This confirms that the piezoelectric sensor analysis is guaranteed to give the correct result (again, for a perfect system) when the creation is instantaneous.

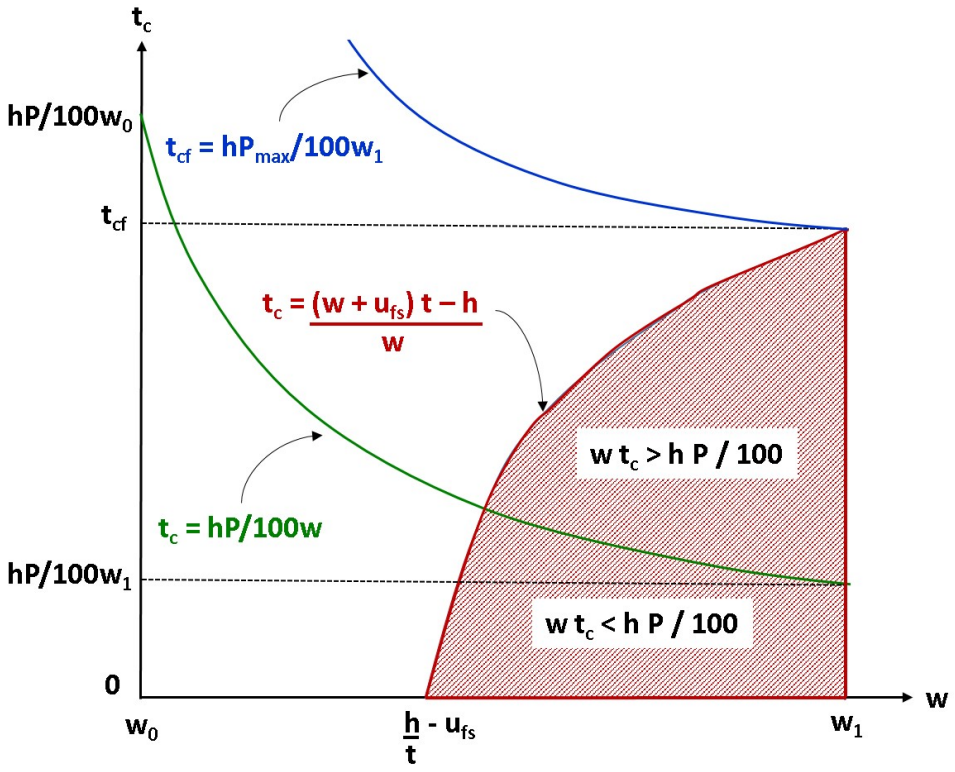

Figure 2: Cartoon depiction of the integration domain for computing $\chi(t)$. The shaded red region is the domain of integration at time t. The green line represents the boundary between $wt_c > \frac{hP}{100}$ and $wt_c < \frac{hP}{100}$ for a given error percentage, P. The error cannot exceed P% unless the green line intersects the domain of integration, as illustrated here (intersection is a necessary but not sufficient condition). The blue line represents the (w, t_c) contour for the largest possible P value, P_{max}. Note this cartoon makes no assertions about the areal mass function $m_c(w, t_c)$, only its domain of integration relevant for $\chi(t)$.

3.2 Stationary velocity distributions

If the ejecta velocity distribution is stationary, then the areal mass function at the source can be written

$$m_c(w, t_c) = f(t_c)g(w).$$

Then the second term of Eqn. 22 becomes

$$\frac{1}{h} \cdot \frac{\int_{\frac{h}{t}-u_{fs}}^{w_1} w\, g(w)\, \mathrm{d}w}{\int_{\frac{h}{t}-u_{fs}}^{w_1} g(w)\, \mathrm{d}w} \cdot \frac{\int_0^{t_c(w,t)} t_c\, f(t_c)\, \mathrm{d}t_c}{\int_0^{t_c(w,t)} f(t_c)\, \mathrm{d}t_c}.$$

When both upper limits of integration are < 1 in the units of the problem, each integral ratio must be less than unity. A detailed study of analytic test problems with stationary velocity distributions confirms that $\chi(t) \approx 1$ in many cases.

3.3 Time-dependent u_{fs}

When u_{fs} is constant, the free surface velocity enters $\chi(t)$ only via the limits of integration in Eqn. 22. If instead u_{fs} is a function of t_c, the resulting nonalgebraic formulation could be considerably different. However, in that case, the true value of $\chi(t)$ may be expected to reside in the range defined by evaluations of Eqn. 22 for the maximum and minimum values of u_{fs} over the ejecta creation period. From dimensional analysis, we expect Eqn. 24 to provide a decent estimate of P_{max}, even for this scenario.

4 Application to Published Shots

Table I lists P_{max} values computed from Eqn. 24 for several shots found in the literature [4, 6].

Experiment	100 ns	500 ns	1.0 μs	1.5 μs	2.0 μs
[4] Shot 5	1.5	7.5	14.9	22.4	29.8
[4] Shot 6	0.3	1.5	3.1	4.6	6.2
[4] Shot 8	1.4	6.9	13.7	20.6	27.5
[4] Shot 10	0.2	1.1	2.3	3.4	4.5
[4] Shot 11	0.2	0.9	1.9	2.8	3.7
[4] Shot 12	0.3	1.6	3.1	4.7	6.2
[6] Target 11	0.2	1.2	2.3	3.5	4.7
[6] Target 12	0.4	1.9	3.9	5.8	7.8

Table I: P_{max} values (%) as a function of t_{cf}, for eight shots selected from the literature. The w_1 and h values are taken from the references, and t_{cf} is treated as a free parameter.

P_{max} rarely exceeds 10% even when the ejecta creation interval, t_{cf}, extends to 2 μs, a duration greatly exceeding "conventional wisdom" of 100-200 ns. In all cases, the upper bound on the error is less than 15% when creation persists for a full microsecond.

If the *aggregate* error in the voltage measurement were to exceed 5%, then in six of the eight cases listed in Table I the piezoelectrically inferred ejecta mass values could not be used to reliably distinguish between creation intervals of 100 ns and 1 μs.

This work is supported by US DOE/NNSA, performed at LANL, operated by LANS LLC under contract DE-AC52-06NA25396.

References

[1] Cherne, F. J., Hammerberg, J. E., Andrews, M. J., Karkhanis, V., and Ramaprabhu, P. "On Shock Driven Jetting of Liquid from Non-Sinusoidal Surfaces into a Vacuum," *J. Appl. Phys.* **118**:185901 (2015).

[2] Buttler, W. T., Oró, D. M., Preston, D. L., Mikaelian, K. O., Cherne, F. J., Hixson, R. S., Mariam, F. G., Morris, C., Stone, J. B., Terrones, G., and Tupa, D., "Unstable Richtmyer-Meshkov growth of solid and liquid metals in vacuum," *J. Fluid Mech.* **703**:60–84 (2012).

[3] Dimonte, Guy, Terrones, Guillermo, Cherne, F. J., and Ramaprabhu, P. "Ejecta source model based on the nonlinear Richtmyer-Meshkov instability," *J. Appl. Phys.* **113**:024905 (2013).

[4] Vogan, W. S., Anderson, W. W., Grover, M., Hammerberg, J. E., King, N. S. P., Lamoreaux, S. K., Macrum, G., Morley, K. B., Rigg, P. A., Stevens, G. D., Turley, W. D., Veeser, L. R., and Buttler, W. T. "Piezoelectric characterization of ejecta from shocked tin surfaces," *J. Appl. Phys.* **98**:113508 (2005).

[5] Zellner, M. B., Grover, M., Hammerberg, J. E., Hixson, R. S., Iverson, A. J., Macrum, G. S., Morley, K. B., Obst, A. W., Olson, R. T., Payton, J. R., Rigg, P. A., Routley, N., Stevens, G. D., Turley, W. D., Veeser, L., and Buttler, W. T. "Effects of shock-breakout pressure on ejection of micron-scale material from shocked tin surfaces," *J. Appl. Phys.* **102**:013522 (2007).

[6] Monfared, S. K., Oró, D. M., Grover, M., Hammerberg, J. E., LaLone, B. M., Pack, C. L., Schauer, M. M., Stevens, G. D., Stone, J. B., Turley, W. D., and Buttler, W. T. "Experimental observations on the links between surface perturbation parameters and shock-induced mass ejection," *J. Appl. Phys.* **116**:063504 (2014).

[7] Buttler, W. T., Oró, D. M., Olson, R. T., Cherne, F. J., Hammerberg, J. E., Hixson, R. S., Monfared, S. K., Pack, C. L., Rigg, P. A., Stone, J. B., and Terrones, G. "Second shock ejecta measurements with an explosively driven two-shockwave drive," *J. Appl. Phys.* **116**:103519 (2014).